ELSEVIER

Journal of Hazardous Materials B105 (2003) 63–81

Journal of Hazardous Materials

www.elsevier.com/locate/jhazmat

Thermal decomposition of 1,1-dichloroethene diluted in hydrogen

Yo-ping G. Wu [a,*], Yang-soo Won [b]

[a] *Department of Chemical and Materials Engineering, National I-Lan University, I-Lan, 26041, Taiwan, ROC*

[b] *Department of Environmental Engineering, Yeungnam University, Kyoungsan City, Kyoungpook 712-749, South Korea*

Received 14 April 2003; accepted 30 June 2003

Abstract

The reaction of 1,1-dichloroethene in an excess hydrogen environment with a Cl/H ratio of 0.04 was investigated in an isothermal tubular reactor at a total pressure of 1 atm with residence time of 0.3–2.0 s between 575 and 900 °C. C_2H_3Cl and HCl are the primary reaction products from the decomposition of CH_2CCl_2 while the formation of C_2H_4, C_2H_2, C_2H_6, and CH_4 increases as reaction time or temperature increases.

Modeling used a detailed chemical mechanism involving 59 species and 202 elementary reactions; the results were compared with experimental observations. Sensitivity analyses were also performed to rank the significance of each reaction in the mechanism. The optimal reaction condition for the C_2 hydrocarbons production from the dechlorination of CH_2CCl_2 in H_2 environment was also determined.

Keywords: Pyrolysis; Ethylene; Dechlorination; Reaction kinetics; Dichloroethene

1. Introduction

Chlorinated organic compounds are widely used in synthesis and in chemical industry. Thermal treatment of these chlorinated hydrocarbons provide a source of chlorine atoms in the initial stages of the process and are thought to be associated with the formation of aromatics such as di-benzo-dioxins and di-benzo-furans in incinerators, and have gained much attention due to the fact that some are toxic and in some cases carcinogenic [1–4].

* Corresponding author. Tel.: +886-3-9357400x702; fax: +886-3-9357025.
E-mail address: ypwu@niu.edu.tw (Y.-p.G. Wu).

0304-3894/$ – see front matter © 2003 Elsevier B.V. All rights reserved.
doi:10.1016/j.jhazmat.2003.06.001

Different technologies have been developed for the safe destruction of chlorinated hydrocarbons. Thermal destruction of organic pollutants in an oxygen-rich atmosphere is the method most often used in the chemical waste disposal industry. It is reported that the combustion of chlorinated hydrocarbons under severe conditions converts all carbon to CO_2 [5,6].

While oxygen is involved in the process, oxygen and Cl are both competing for the available fuel hydrogen and this is one reason that chlorinated hydrocarbons serve as flame inhibitors [7]. Also, C–Cl may persist in an oxygen-rich system of limited hydrogen atmosphere [5,8], as the emission of toxic chlorinated organic products persists through an oxygen rich incineration in which carbon species is one of the more stable sinks for the chlorine.

To obtain a quantitative formation of HCl as one of the desired and thermochemically favorable products from chlorinated hydrocarbons, one might use a straightforward thermal conversion of these compounds under a more reductive atmosphere of hydrogen. The "non-oxygen" methods were developed in order to avoid the formation of undesired oxy-containing products, such as phosgene and dioxins. The chlorocarbons and hydrogen system contains only C, H, and Cl elements and is expected to lead to the formation of light hydrocarbons and hydrogen chloride at the temperatures where complete reaction occurs. Under such a system, carbon can be converted to CH_4, C_2H_2, C_2H_4 and C_2H_6 [9,10].

Louw et al. [6] studied a series of reactions on chlorinated benzenes, alkenes, and alkanes with hydrogen. They reported that the pyrolysis process under a sufficient amount of H_2 is a feasible method for dechlorination of organic chlorine compounds. They also pointed out that the product may be used as a fuel or raw material after trapping HCl.

Manion and Louw [10] studied the gas-phase hydrogenolysis of vinyl chloride in a tubular flow reactor at atmospheric pressure between 872 and 1085 K. They reported that the C_2H_4, C_2H_2, and HCl are the major initial products of the reaction. They also investigated the effects of addition of HCl and reported that the addition of HCl increased the C_2H_3Cl conversion at low temperatures by about a factor of two.

Taylor et al. [11] studied the high temperature, oxygen-free pyrolysis of C_2Cl_4 from 573 to 1273 K using tubular flow reactors. They reported that the reaction products included C_2Cl_2, Cl_2, CCl_4, hexachlorobutadiene (C_4Cl_6), and hexachlorobenzene (C_6Cl_6). They also presented the effects of reactor surface area to volume (S/V) ratio on the initial decomposition of C_2Cl_4.

Tsang and Walker [12] studied the hydrogen atom attack on C_2Cl_4 under high-temperature conditions in a single pulse shock tube. They reported the rate constants for the abstraction reaction: $H + C_2Cl_4 \rightarrow C_2Cl_3 + HCl$, and the displacement reaction: $H + C_2Cl_4 \rightarrow C_2HCl_3 + Cl$.

As part of a series of the analyses of chlorinated hydrocarbons in hydrogen-rich environment [13,14], this study was performed in a tubular flow reactor to examine the pyrolysis of CH_2CCl_2 with H_2, in a non-oxidative environment. We characterize the reactant loss, intermediate distribution, and product formation as functions of time and temperature to describe the reaction process, and to investigate the feasibility of the formation of the light hydrocarbons, e.g. C_2H_4 or C_2H_6, from the reaction of chlorinated ethylene in this study.

2. Experimental method

The experimental apparatus and the procedures used in this study are similar to those used in our earlier studies [13–16]. Therefore, only a brief summary of these subjects is given. Pure 1,1-dichlorethene (CH_2CCl_2) was reacted with hydrogen (in the absence of O_2) in an isothermal tubular reactor at 1 atm. The products of this thermal degradation were analyzed systematically by varying the temperature from 575 to 900 °C and the residence time from 0.3 to 2.0 s.

Hydrogen gas was passed through a multi-saturator train held at 0 °C to ensure saturation with CH_2CCl_2 in order to accurately calculate the vapor pressure. A second stream of hydrogen diluted the flow of $CH_2CCl_2 + H_2$ to achieve the desired mole fraction. The ratio of the mole fraction of CH_2CCl_2 to hydrogen was 1:24, which gives Cl/H = 0.04. The reagent and hydrogen were preheated to 200 °C and fed continuously into the reactor.

The quartz tubular reactor (i.d. = 8 mm) was housed within a three-zone electrical furnace (length = 81.3 cm) equipped with three independent temperature controllers. Temperature profiles were obtained using a type K thermocouple moved axially within the reactor under representative flow conditions. Tight control resulted in temperature profiles constant to within ±3 °C over 75% of the furnace's length.

The effluent from the reactor was passed through transfer lines, heated to 170 °C to limit condensation, to the GC gas sampling valve and exhaust. An on-line GC (HP 5890) with FID was used to identify the products. The GC used a 1.5 m × 3.2 mm stainless steel column packed with 1% Alltech AT-1000 on Graphpac-GB.

Quantitative analysis of HCl was performed for each run. The samples for HCl analysis were collected independently from the GC sampling line. The effluent from the reactor was diverted through a two-stage bubbler containing 0.01 M aqueous NaOH before being exhausted to a fume hood. The concentration of HCl in the effluent was then calculated after titrating the solution with 0.01 M HCl to its phenolphthalein end point.

3. Results and discussion

3.1. Decay of chloroethylenes

Examples of the experimental results for the decomposition of CH_2CCl_2 (DCE) in this study are presented, in Fig. 1(a), which shows a normalized concentration ($[DCE]/[DCE]_0$) as a function of temperature at 1.0 s residence time. As shown in Fig. 1(a), DCE concentration consistently decreased with increasing temperatures and reaction times in this reaction system. The thermal stability (defined by the temperature required for 99% destruction after a reaction time of 1 s) of CH_2CCl_2 was determined to be 825 °C in this study.

An integrated rate equation plot for the conversion of CH_2CCl_2 to fit a first order rate equation was made in Fig. 1(b). The activation energy and Arrhenius frequency factor for the global reaction (loss) of CH_2CCl_2 in this study was found from the Arrhenius plot as shown in Fig. 1(c). The global Arrhenius equation of CH_2CCl_2 from this study is: $k = 4.95 \times 10^{22} \exp(-52.9 \times 10^3/T)$ (s^{-1}).

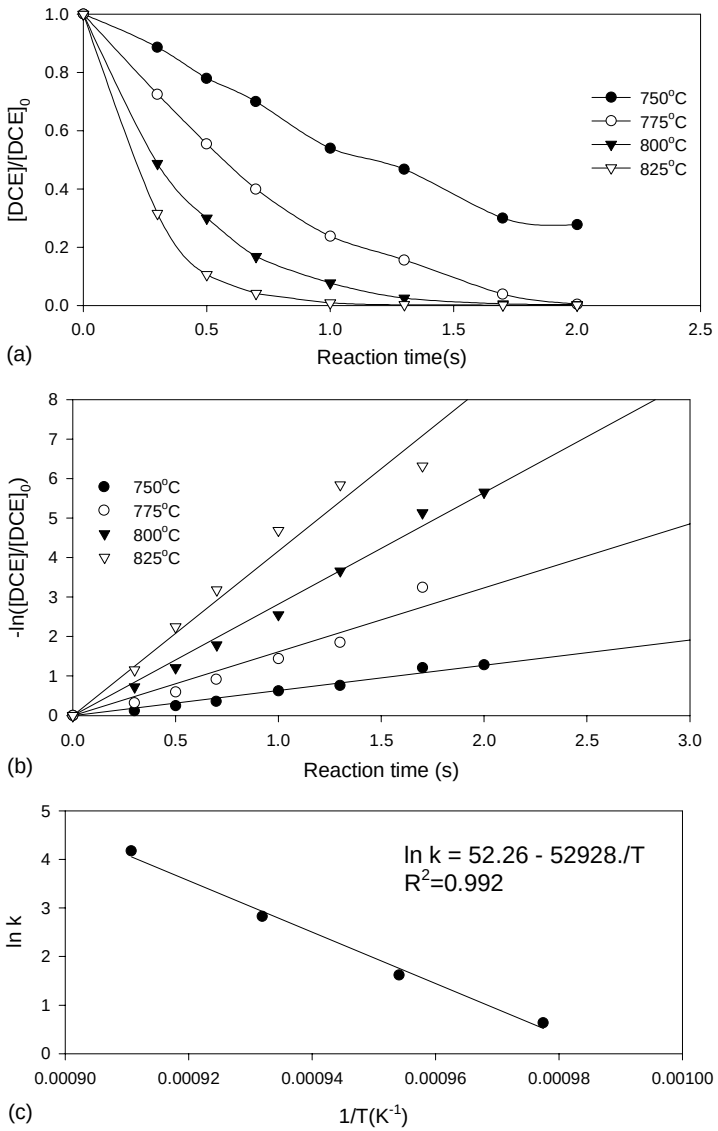

Fig. 1. The decomposition of 1,1-DCE. (a) Normalized concentration (C/C_0) distributions of 1,1-DCE as a function of temperature at 1.0 s reaction time, (b) Integrated rate equation plot for the conversion of DCE, and (c) The global Arrhenius plot.

Table 1 presents the product distributions identified by the GC and HCl analyses for this reaction system as a function of temperature at 1.0 s reaction time. Fig. 2 shows the profiles of the reactant and products at 750 °C as functions of reaction time. As shown in Fig. 2 along with Table 1, C_2H_3Cl, C_2H_4, C_2H_2, C_2H_6, CH_4, and HCl are the major products for the

Table 1
Material balance of carbon and chlorine in CH_2CCl_2/H_2 reaction system at reaction time = 1.0 s

Species	Mole (%) at different reaction temperatures (°C)								
	650	700	725	750	800	825	850	875	900
CH_4	ND	ND	ND	*	**	**	***	+	+
C_2H_2	ND	*	*	**	+	+	**	**	**
C_2H_4	ND	*	**	+	++	++	++	++	++
C_2H_6	ND	ND	*	**	+	+	+	+	+
C_2HCl	*	*	*	*	*	*	*	*	*
C_2H_3Cl	**	***	+	++	***	**	*	ND	ND
CH_2Cl_2	ND	ND	*	*	*	ND	ND	ND	ND
C_4H_{10}	ND	ND	*	*	*	*	*	*	*
CH_2CCl_2	++++	++++	+++	++	***	*	*	*	*
CHClCHCl	ND	ND	*	*	*	ND	ND	ND	ND
C_6H_6	ND	ND	ND	**	**	**	**	**	***
C_6H_5Cl	ND	ND	ND	ND	*	*	**	ND	ND
HCl	**	***	+	++	+++	+++	+++	+++	+++
Total C (mole (%))	99.7	98.6	94.7	102.5	101.2	91.2	94.7	98.8	104.5
Total Cl (mole (%))	101.44	105.43	106.5	112.7	93.38	83.2	81.09	81.36	78.37

ND < 0.1 < * < 1 < ** < 5 < *** < 10 < + < 25 < ++ < 60 < +++ < 90 < +++ < 100 mole (%).

reaction of CH_2CCl_2 diluted in H_2 in this study. Among these species, C_2H_3Cl and HCl are the primary reaction products from the decomposition of CH_2CCl_2, while the formation of C_2H_4, C_2H_2, C_2H_6, and CH_4 increased as reaction time or temperature increased. Some minor intermediate reaction products, including C_2HCl, CH_2Cl_2, CHClCHCl, C_4H_{10}, C_6H_6, and C_6H_5Cl, were found from the experimental data of this study. Table 1 also shows an example of the material balances of carbon and chlorine performed in this study. Taking into

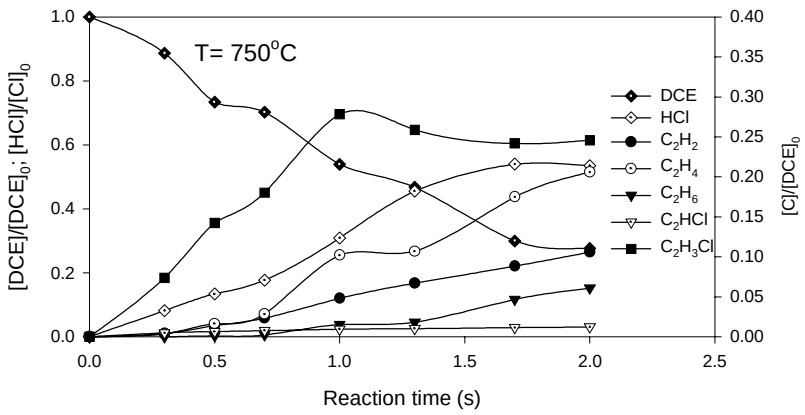

Fig. 2. Normalized concentration (C/C_0) profiles of 1,1-DCE, C_2H_3Cl, C_2H_2, C_2H_4, C_2H_6, CHCCl and HCl as a function of reaction time at 750 °C.

account the uncertainty of experimental analyses, most of the carbon and chlorine balances show acceptable results (>78%). The formation pathways for these intermediate species will be discussed with the modeling results in the next section.

3.2. Results of modeling and reaction pathway analysis

The mechanism that we used in this study consists of 59 species and 202 elementary reactions, including C_1 and C_2 species, and is based on the mechanism described detail by Wu and Won [13], and Wu et al. [14]. Recommended rate parameters were used, as well as direct experimental measurements, whenever possible [17–19]. The rate parameters and thermochemical properties of the elementary reactions with the elements C/H only were mainly adopted directly from the GRI-Mech Version 3.0 [20]. Elementary reaction rate parameters for abstraction reactions were based upon literature comparison, thermodynamic estimations, and the Transition State Theory methods of Benson [21]. The computer code CHEMACT [22] was used to calculate the parameters for the unimolecular reactions and the chemical activation reactions. The CHEMKIN-II [23] suite of numerical integration codes was used for calculating actual rates of reaction. All the thermochemical information, including the heats of formation, specific entropies, and the temperature-dependent specific heats, were taken from available sources, such as the JANAF Thermochemical Tables [24], Stull et al. [25], GRI-Mech [20], and Pedley et al. [26]. THERM [27] was used to calculate the thermal properties for some of the species in mechanism.

A comparison of the calculated concentrations with experimental values is shown in Figs. 3–5. The curves come from modeling and the symbols are the experimental measurements. Fig. 3 is for the comparison of CH_2CCl_2 and HCl species as a function of temperature at 1.0 s residence time (Fig. 3a) and as a function of reaction time at 800 °C (Fig. 3b). This figure shows that the modeling of the decay of CH_2CCl_2 is in good agreement with the experiment. The mechanism shows a good prediction on the concentration of HCl for temperatures lower than 775 °C at 1.0 s reaction time or for reaction times less than 1.0 s at 800 °C. However, the model then over-predicts the concentration of HCl. Fig. 4 compares the modeling result with the experiment for C_2H_3Cl and CH_4 as a function of temperature at 1.0 s residence time (Fig. 4a), and as a function of reaction time at 800 °C (Fig. 4b). As shown in both figures, the model prediction matches the experimental results for C_2H_3Cl. The model also gives a good prediction on the formation of CH_4, except in the cases of higher temperatures. Comparisons of model and experiment for C_2H_4, C_2H_2, and C_2H_6 are shown in Fig. 5(a) for 1.0 s residence time and in Fig. 5(b) at 800 °C. As illustrated in both figures, the agreement between model and experiment for the concentrations of these species is reasonable. The possible routes for C_2H_3Cl formation are the replacement reaction, $CH_2CCl_2 + H \rightarrow C_2H_3Cl + Cl$, or the abstraction reaction of $CH_2CCl^{\bullet}$ radical abstract H from H_2 leading to C_2H_3Cl. The dissociation reaction, $CH_2CCl_2 \rightarrow CH_2CCl + Cl$, and abstraction reaction, $CH_2CCl_2 + H \rightarrow CH_2CCl + HCl$, can both result in a $CH_2CCl^{\bullet}$ radical.

Hydrogen atom addition to the substituted end of C_2H_3Cl (yielded from the reactions of CH_2CCl_2) and the loss of a chlorine atom from the radical intermediate, or replacement reaction, $C_2H_3Cl + H \rightarrow C_2H_4 + Cl$, can both lead to the formation of C_2H_4. The HCl elimination reaction of C_2H_3Cl can give the formation of C_2H_2. The abstraction reaction

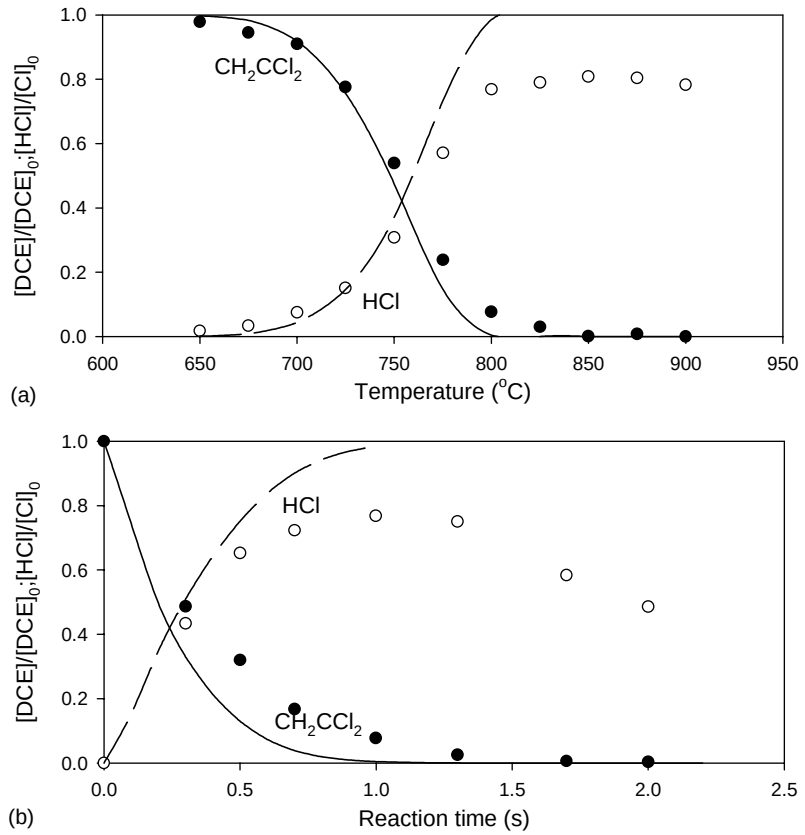

Fig. 3. Comparison of experimental data with model prediction for 1,1-DCE and HCl. (a) Reaction time = 1.0 s and (b) reaction temperature = 800 °C.

of C_2H_3Cl by H can also lead to the formation of a vinyl radical, which may lose H to produce C_2H_2. C_2H_6 can then be produced through the hydrogenation of C_2H_4. The possible pathway for the formation of CH_4 is through the H abstraction of CH_3 from H_2 or HCl, where the CH_3 can be formed from the bond fission of C_2H_6.

3.3. Sensitivity analysis

Sensitivity analyses were also performed to identify the rank order of significance of each reaction in the mechanism for this reaction system. The Sandia program SENS [28] was used to obtain the first-order sensitivity coefficients with respect to their rate parameters. The following Figs. 6–10 present the results of the sensitivity analysis of the major species, CH_2CCl_2, C_2H_3Cl, C_2H_2, C_2H_4, and C_2H_6, in this reaction system as a function of temperature and as a function of reaction time. Table 2 summarized the most important reactions with the rate parameters and heats of reaction (ΔH) for the forward reaction

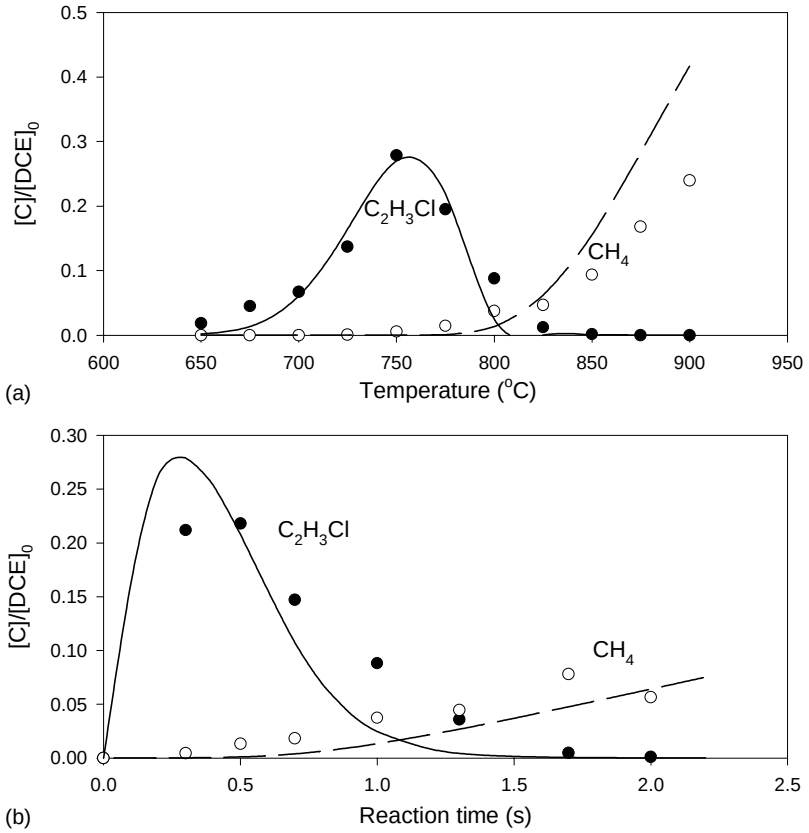

Fig. 4. Comparison of experimental data with model prediction for C_2H_3Cl and CH_4. (a) Reaction time = 1.0 s and (b) reaction temperature = 800 °C.

paths for these five species into 20 reactions. Thus, Fig. 6 presents the sensitivity coefficients for the 10 most important reactions for CH_2CCl_2 at reaction time 1.0 s and at 700 and 750 °C. As seen in Fig. 6(a), the dissociation reaction, $CH_2CCl_2 \rightarrow CH_2CCl + Cl$; the H abstraction reaction, $CH_2CCl_2 + H \rightarrow CH_2CCl + HCl$; and the replacement reaction, $CH_2CCl_2 + H \rightarrow C_2H_3Cl + Cl$ are the primary reactions for the decomposition of CH_2CCl_2. Further inspection of the results in Fig. 6(a) shows that the dissociation reaction $CH_2CCl_2 \rightarrow CH_2CCl+Cl$ is the most sensitive reaction in the lower temperature range, and the same phenomena can be found from the curves shown in Fig. 6(b) and (c). The sensitivity coefficient curves in Fig. 6(b) and (c) show similar important channels at different temperatures and show that the abstraction reaction, $CH_2CCl_2 + H \rightarrow CH_2CCl + HCl$, becomes competitive with the dissociation reaction, $CH_2CCl_2 \rightarrow CH_2CCl+Cl$, as temperatures rise. Fig. 6 also suggests that the important reaction channels, e.g. $CH_2CCl_2 \rightarrow C_2HCl + HCl$ and $CCl_2CH \rightarrow C_2HCl+Cl$, are related to the formation of C_2HCl, or, $2CH_3 \rightarrow C_2H_6$ and $2CH_3 \rightarrow H + C_2H_5$ for the production of CH_4 and C_2H_6 species. The sensitivity analysis of these species will be further discussed below.

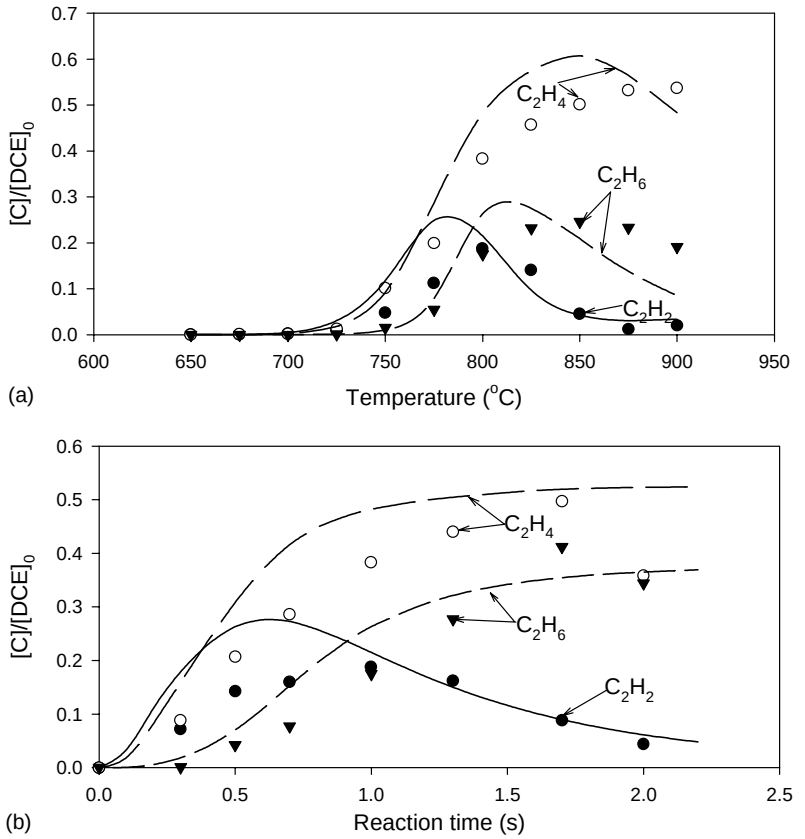

Fig. 5. Comparison of experimental data with model prediction for C_2H_2, C_2H_4 and C_2H_6. (a) Reaction time = 1.0 s and (b) reaction temperature = 800 °C.

The sensitivity coefficients for the 10 most important reactions for C_2H_3Cl are shown in Fig. 7. Fig. 7(a) shows the sensitivity coefficients for C_2H_3Cl as a function of temperature at reaction time 1.0 s. As shown in Fig. 7(a), the primary reactions for the decay of the reactant $CH_2CCl_2 \rightarrow CH_2CCl + Cl$, $CH_2CCl_2 + H \rightarrow CH_2CCl + HCl$, and $CH_2CCl_2 + H \rightarrow C_2H_3Cl + Cl$ consistently show the highest sensitivities for C_2H_3Cl in the lower temperature range. The other reactions: $C_2H_3Cl + H \rightarrow C_2H_4 + Cl$, $C_2H_3Cl + H \rightarrow C_2H_3 + HCl$, and $CH_3CCl_2 + H \rightarrow C_2H_3Cl + HCl$ also become important with increasing temperature. Fig. 7(b) shows the sensitivity coefficients at 800 °C for the same 10 reactions. As observed from this figure, $C_2H_3Cl + H \rightarrow C_2H_4 + Cl$ becomes the favorite channel responsible for the decomposition of C_2H_3Cl for reaction time longer than 0.3 s. There are two reactions, $H + C_2H_5 \rightarrow C_2H_6$ and $2CH_3 \rightarrow C_2H_6$, which also have high-sensitivity coefficients under this reaction condition, and which were mainly caused by the production of C_1 or C_2 hydrocarbons in this range.

Fig. 8(a) presents the sensitivity coefficients for the 10 most important reactions for C_2H_2 as a function of temperature at reaction time 1.0 s. The reactions: $CH_2CCl_2 \rightarrow CH_2CCl + Cl$,

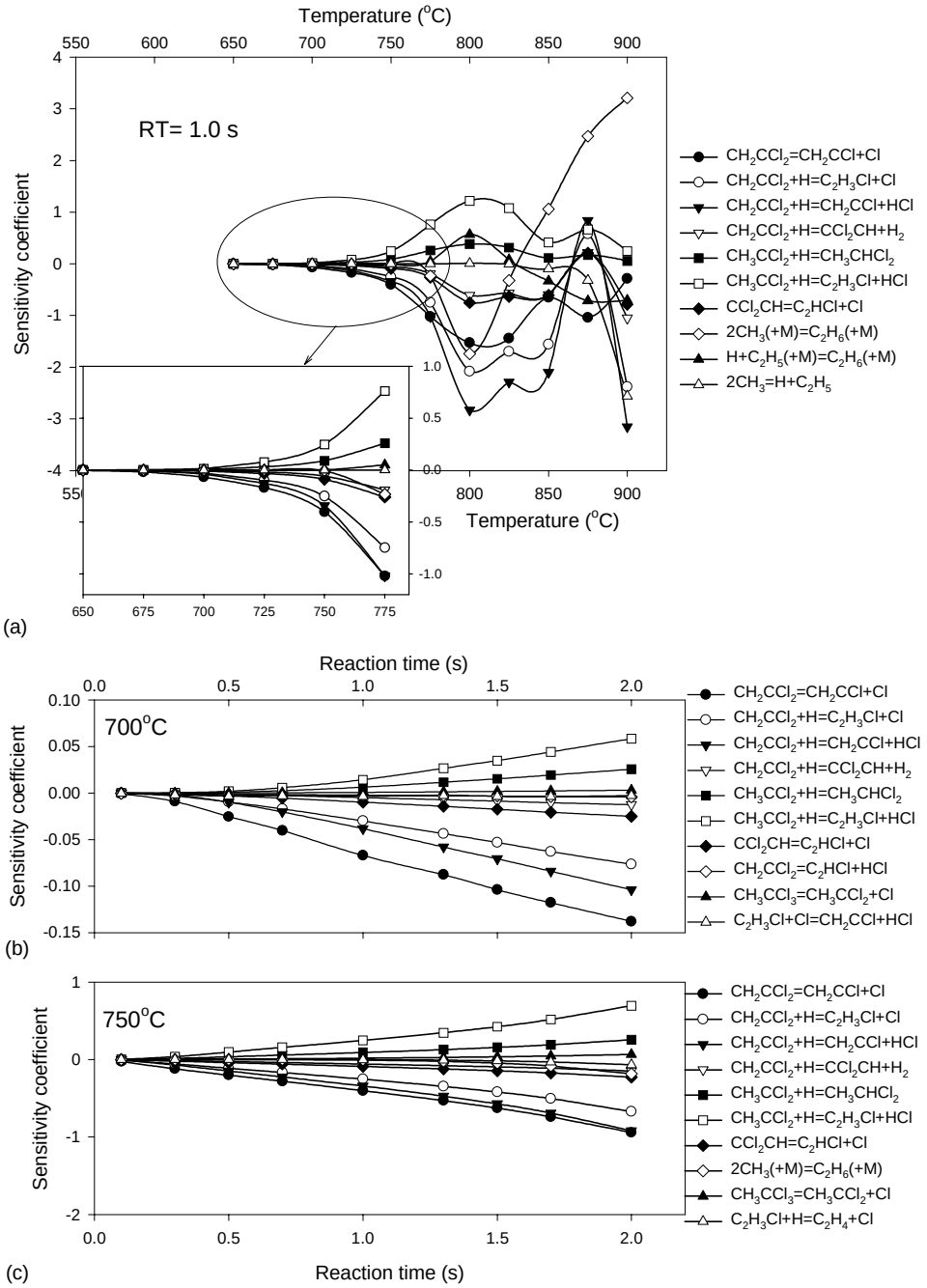

Fig. 6. Ten most important reactions for DCE and their sensitivity coefficients. (a) Reaction time = 1.0 s, (b) reaction temperature = 700 °C, and (c) 750 °C.

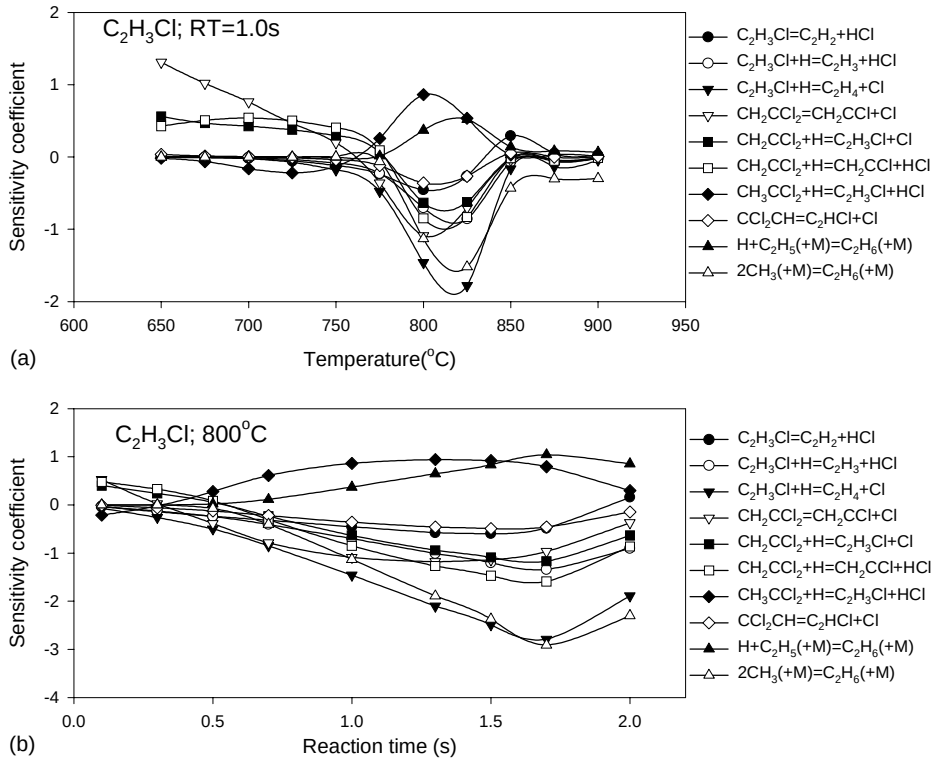

Fig. 7. Ten most important reactions for C_2H_3Cl and their sensitivity coefficients. (a) Reaction time = 1.0 s and (b) reaction temperature = 800 °C.

$CH_2CCl_2 + H \rightarrow CH_2CCl + HCl$, and $CH_2CCl_2 + H \rightarrow C_2H_3Cl + Cl$, as discussed above, are also sensitive to the source species for reaction. The reactions: $C_2H_3Cl \rightarrow C_2H_2 + HCl$, $C_2HCl + H \rightarrow C_2H_2 + Cl$, $C_2H_3Cl + H \rightarrow C_2H_4 + Cl$, $CH_3CCl_2 + H \rightarrow C_2H_3Cl + HCl$, $CCl_2CH \rightarrow C_2HCl + Cl$, $H + C_2H_2 \rightarrow C_2H_3$, and $2CH_3 \rightarrow C_2H_6$ have high sensitivity in this system. The sensitivity coefficients for C_2H_2 as a function of reaction time at 800 °C for the same 10 reactions are shown in Fig. 8(b). There are two groups important to these 10 reactions. In the first group, most of the reactions in Fig. 8(b) show that the high-sensitivity coefficients are not related to the reaction times. Second group, $H + C_2H_2 \rightarrow C_2H_3$ and $2CH_3 \rightarrow C_2H_6$, not only shows their high sensitivity but also shows the effect of a changing reaction time.

The sensitivity coefficients for the 10 most important reactions for C_2H_4 as a function of temperature at 1.0 s are shown in Fig. 9(a). The difference between the sensitivity coefficients of these 10 reactions is easily observed for temperatures lower than 800 °C, and the reactions responsible for the decomposition of CH_2CCl_2 and C_2H_3Cl retain their high sensitivity. However, the curves of the sensitivity coefficients merge into two main regions and suggest that $2CH_3 \rightarrow H + C_2H_5$ and $2CH_3 \rightarrow C_2H_6$ dominate for temperatures higher than 800 °C. The sensitivity coefficients for the 10 most important reactions for C_2H_4 as function of

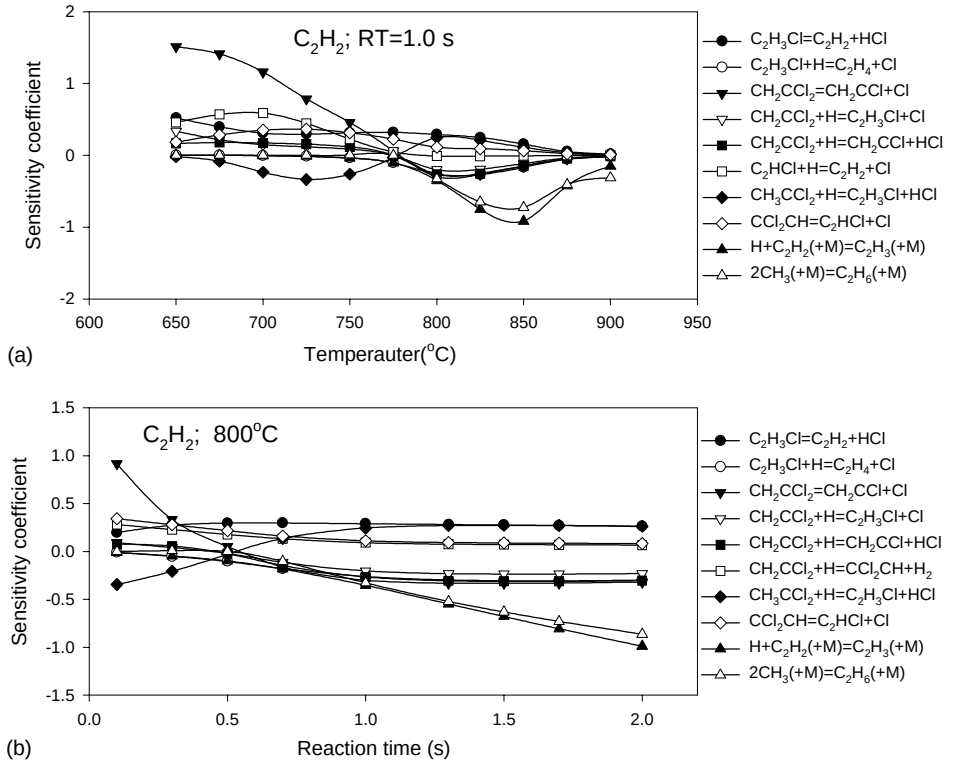

Fig. 8. Ten most important reactions for C_2H_2 and their sensitivity coefficients. (a) Reaction time = 1.0 s and (b) reaction temperature = 800 °C.

reaction time at 700, 750, and 800 °C are shown in Fig. 9(b)–(d), respectively. The curves of the sensitivity coefficients in Fig. 9(b) show that the dissociation reaction of CH_2CCl_2, $CH_2CCl_2 \rightarrow CH_2CCl + Cl$, is the most dominating reaction at lower temperature, such as at 700 °C as shown in Fig. 9(b). As shown in Fig. 9(c) and (d), the differences between the sensitivity coefficients decreases with increasing temperature. Also, as with the results shown in Fig. 9(a), the hydrocarbon formation channels, $H + C_2H_2 \rightarrow C_2H_3$ and $2CH_3 \rightarrow C_2H_6$, become important with increasing temperature.

The sensitivity coefficients for the 10 most important reactions for C_2H_6 as a function of temperature at 1.0 s are shown in Fig. 10(a), and the coefficients as a function of reaction time at 800 °C are shown in Fig. 10(b). As with the previous figures of the sensitivity coefficients, the dominant reactions for the decomposition of CH_2CCl_2 and C_2H_3Cl show a consistently high sensitivity here. The reactions $H + C_2H_4 \rightarrow C_2H_5$ and $2CH_3 \rightarrow C_2H_6$ are also important. The shape of the curves shown in Fig. 10(a) is also similar to those in Fig. 9(a), which merged to two regions for temperatures higher than 825 °C, and $2CH_3 \rightarrow C_2H_6$ is the most dominant channel. The curves shown in Fig. 10(b) suggest that the dechlorination reactions dominate at an earlier stage of the reaction under a higher temperature environment. The sensitivity coefficients of these reactions decrease with increasing reaction time and the

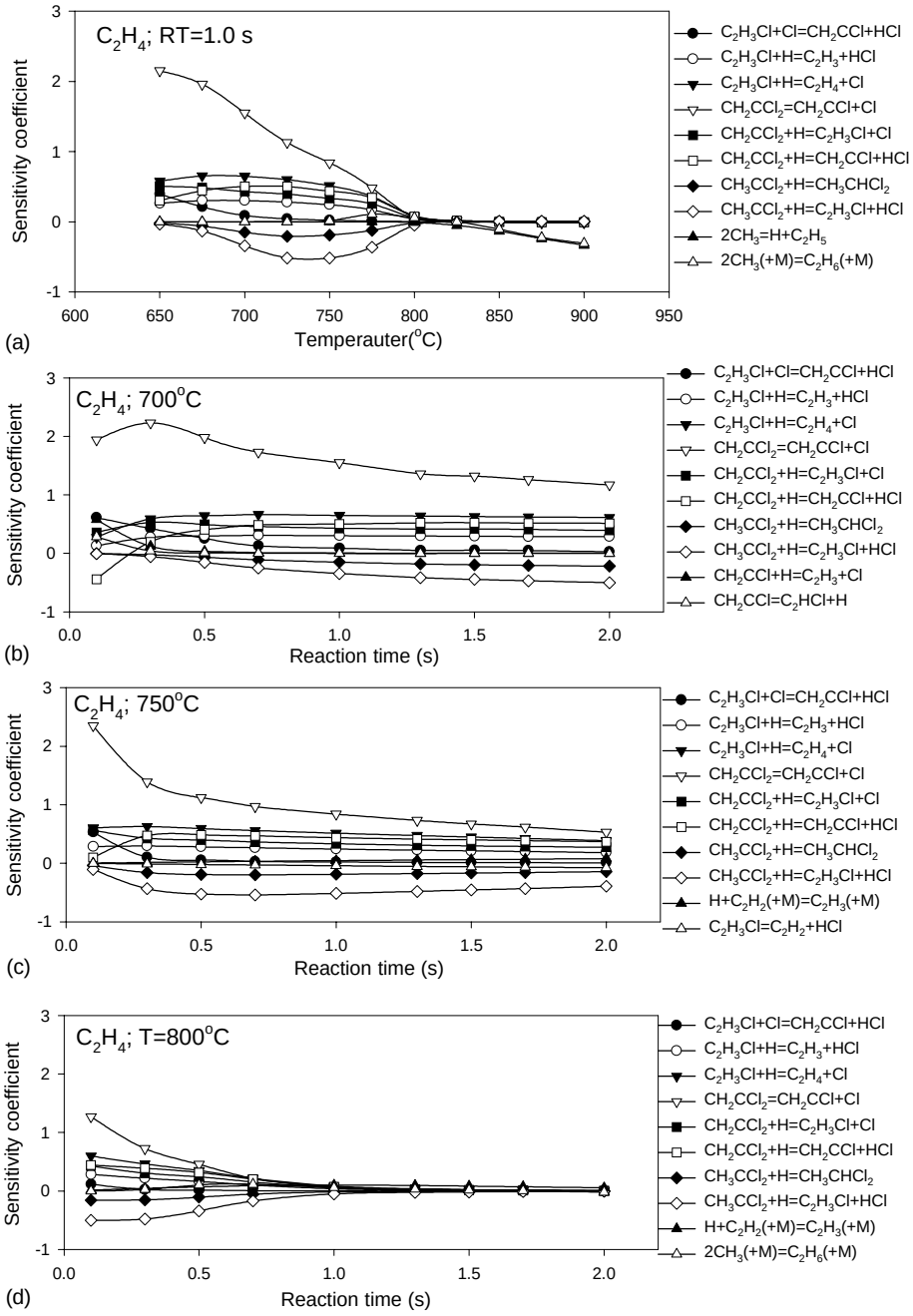

Fig. 9. Ten most important reactions for C_2H_4 and their sensitivity coefficients. (a) Reaction time = 1.0 s, (b) reaction temperature = 700 °C, (c) 750 °C, and (d) 800 °C.

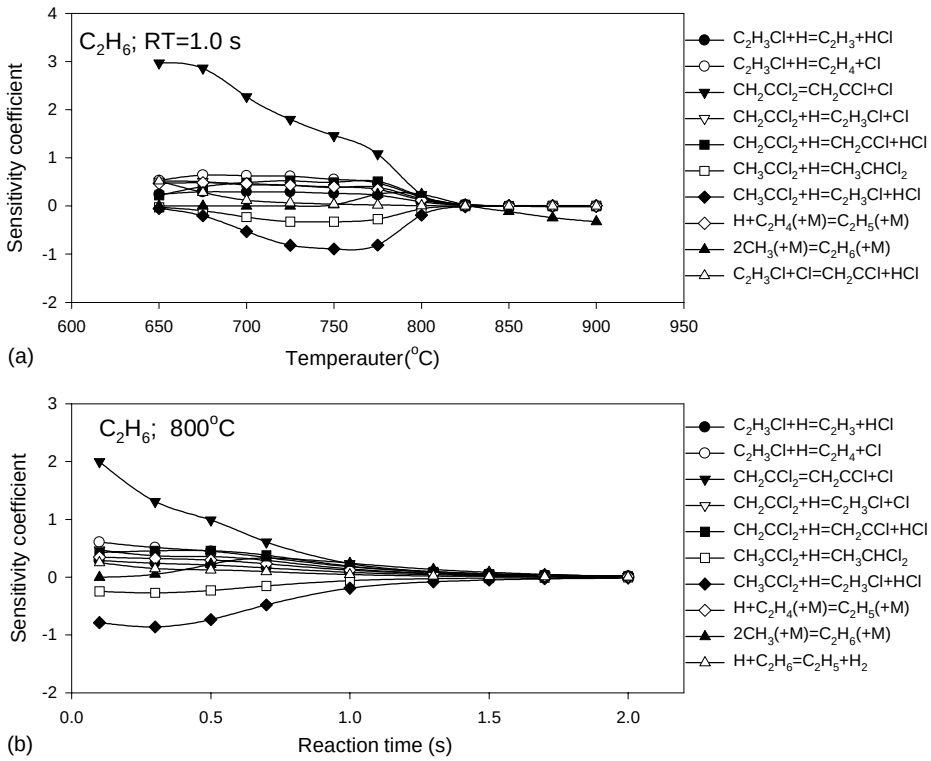

Fig. 10. Ten most important reactions for C_2H_6 and their sensitivity coefficients. (a) Reaction time = 1.0 s and (b) reaction temperature = 800 °C.

reactions containing only hydrocarbon species become important and compete with these dechlorination reactions.

Figure 11 shows the calculation results of the mechanism for the production of light hydrocarbons, C_2H_4 (Fig. 11a), C_2H_2 (Fig. 11b), C_2H_6 (Fig. 11c), and CH_4 (Fig. 11d), as a function of temperature. It is seen from Fig. 11(a), the formation of C_2H_4 reaches the highest production at 875 °C and 0.5 s, however, the production of C_2H_4 can reach over 50% of the reactant at 800 °C if reaction time is long enough (e.g. 3.0 s in this case). Fig. 11(b) shows that the formation of C_2H_2 reaches its highest at 800 °C and 0.5 s, but that the maximum production of C_2H_2 is not much different for different reaction conditions. Also, the maximum C_2H_2 can be formed at lower temperatures if in a long reaction time. As shown in Fig. 11(c), the temperature for the highest formation of C_2H_6 decreased as the reaction time increased. As shown in Fig. 11(d), the formation of CH_4 increased with a temperature or reaction time increase.

The mechanism also was used to simulate different reactant input conditions to find the optimal condition for the production of C_2 hydrocarbons. Here, we have assumed that the effect of reaction, which includes more than three carbons number, is not significant and hence are ignored. There are seven input ratios of the reactants DCE:H_2 = 1:24, 1:15, 1:9,

Table 2
Summary of the rate expressions for the 20 most important reactions for CH_2CCl_2/H_2 with each rate constant of the form $AT^n \exp(-E/RT)$

	Reactions	A	n	E (kJ/mol)	ΔH (kJ/mol)	References
1	$CH_2CCl_2 \rightarrow C_2HCl + HCl$	4.10E+13	0	304.2	119	[13,14]
2	$CH_2CCl_2 \rightarrow CH_2CCl + Cl$	1.40E+14	0	341.8	371.2	[13,14]
3	$CH_2CCl_2 + H \rightarrow C_2H_3Cl + Cl$	1.00E+13	0	24.3	−78.7	[13,14]
4	$CH_2CCl_2 + H \rightarrow CH_2CCl + HCl$	1.20E+13	0	23.0	−60.1	[13,14]
5	$CH_2CCl_2 + H \rightarrow CCl_2CH + H_2$	1.58E+13	0	25.1	23.1	[13,14]
6	$C_2H_3Cl \rightarrow C_2H_2 + HCl$	7.64E+33	−6.3	303.4	114.9	[13,14]
7	$C_2H_3Cl + Cl \rightarrow CH_2CCl + HCl$	3.00E+13	0	23.0	18.6	[13,14]
8	$C_2H_3Cl + H \rightarrow C_2H_3 + HCl$	1.00E+13	0	27.2	−31.5	[13,14]
9	$C_2H_3Cl + H \rightarrow C_2H_4 + Cl$	2.92E+13	−0.1	24.7	−65.5	[13,14]
10	$CCl_2CH \rightarrow C_2HCl + Cl$	5.03E+30	−6.3	91.1	91.2	[13,14]
11	$CH_2CCl + H \rightarrow C_2H_3 + Cl$	1.02E+14	0	0.3	−50.1	[13,14]
12	$C_2HCl + H \rightarrow C_2H_2 + Cl$	2.00E+13	0	8.8	−82.7	[13,14]
13	$CH_3CCl_2 + H \rightarrow CH_3CHCl_2$	5.93E+10	0	−31.6	−395.4	[13,14]
14	$CH_3CCl_2 + H \rightarrow C_2H_3Cl + HCl$	4.69E+12	0	−2.9	−336.7	[13,14]
15	$H + C_2H_2(+M) \rightarrow C_2H_3(+M)$	5.60E+12	0	10.0	−146.4	[20]
16	$H + C_2H_4(+M) \rightarrow C_2H_5(+M)$	5.40E+11	0.5	7.6	−151.8	[20]
17	$H + C_2H_5(+M) \rightarrow C_2H_6(+M)$	5.21E+17	−1	6.6	−420.5	[20]
18	$H + C_2H_6 \rightarrow C_2H_5 + H_2$	1.15E+08	1.9	31.5	−15.5	[20]
19	$2CH_3(+M) \rightarrow C_2H_6(+M)$	6.77E+16	−1.2	2.7	−377.6	[20]
20	$2CH_3 \rightarrow H + C_2H_5$	6.84E+12	0.1	44.4	42.8	[20]

The unit of A are $cm^3/mol\,s$ for bimolecular reaction; s^{-1} for unimolecular reaction.

1:4, 1:3, 1:2, and 1:1 used in this analysis, which result in Cl/H = 0.04, 0.0625, 0.1, 0.2, 0.25, 1/3, and 0.5, respectively. The concentration profiles of DCE, C_2H_4, C_2H_2, C_2H_6, and CH_4 from the model prediction as a function of temperature at 2.0 s, and as a function of reaction time at 825 °C are presented in Fig. 12. As shown in Fig. 12(a), the difference of the ratio of Cl to H in the decomposition of DCE is not significant at temperatures lower than 800 °C, and the effect is observed at temperatures above 800 °C. At higher temperatures, the rate of the decomposition of DCE decreased as the Cl/H ratio increased, but the differences are in tenths of order of magnitude. The formation of C_2H_4 increased with increasing temperatures in most cases and the optimal formation of C_2H_4 can be found in the Cl/H = 0.25 case at 850 °C. Also, in cases with Cl/H ≤ 0.25, the formation of C_2H_4 follows the trends of values of Cl/H and then decreases in the Cl/H = 1/3 and 0.5 cases as shown. The formation of C_2H_2 increased with increasing values of Cl/H, and the Cl/H = 0.5 case presents the highest production in this analysis. For the cases with higher Cl/H value, the C_2H_2 remained at a relatively stable level in a higher temperature range. The formation curves of C_2H_6 all show a peak shape and a decrease in the production of C_2H_6 as Cl/H increased. Cl/H = 0.04, the reaction condition of this study, showed the highest production of C_2H_6 at 800 °C and 2.0 s. The trends on the formation of CH_4 were similar to those of C_2H_6, in which the lower value of Cl/H yielded the higher CH_4 production, but the quantity of CH_4 increased as the reaction temperature increased.

The relationship between Cl/H, the decay of DCE, and the production of hydrocarbons is shown in Fig. 12(b) as a function of reaction time at 825 °C. As with the results as a function

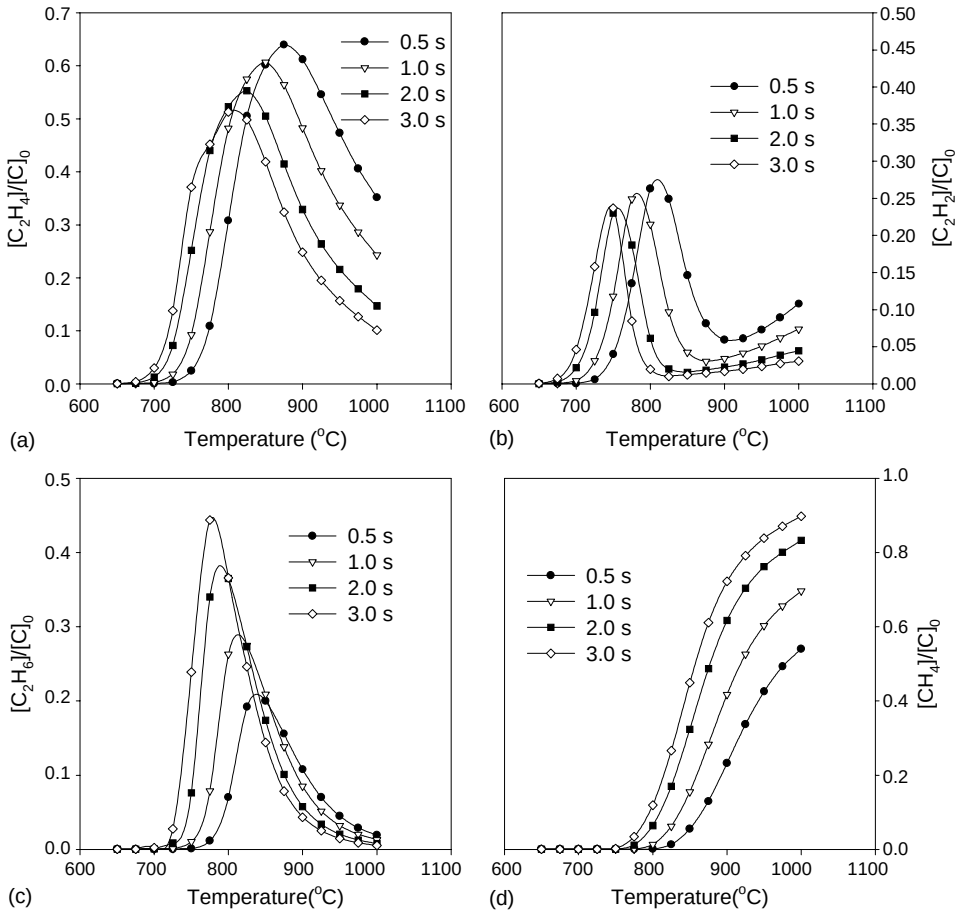

Fig. 11. The calculation profiles of light hydrocarbons as a function of temperature for reaction time = 0.5, 1.0, 2.0, and 3.0 s. (a) C_2H_4, (b) C_2H_2, (c) C_2H_6, and (d) CH_4.

of temperature as shown in Fig. 12(a), the effect of the difference of Cl/H on the decay of DCE is not significant in a shorter reaction time range. The formation of C_2H_4 showed a more complicated situation with the difference of Cl/H. For reaction times within 1.0 s, the reaction with lower Cl/H yielded a higher production of C_2H_4. For reaction times longer than 1.0 s, the concentration of C_2H_4 decreased as reaction time increased in the three cases, Cl/H = 0.04, 0.0625 and 0.1. In the other cases, the formation of C_2H_4 remained steady or increased at a stable rate, and the Cl/H = 0.25 case gave the highest production of C_2H_4 for reaction times longer than 2.0 s. The prediction results of C_2H_2 as a function of reaction time show that the higher value of Cl/H causes a higher and more stable production of C_2H_2. The predictions on the C_2H_6 and CH_4 all show that the higher value of Cl/H yields a higher production of C_2H_6 and CH_4. Among the results of Fig. 12(a) and (b), one can observe that temperature is more important than reaction time for optimal condition determination. From

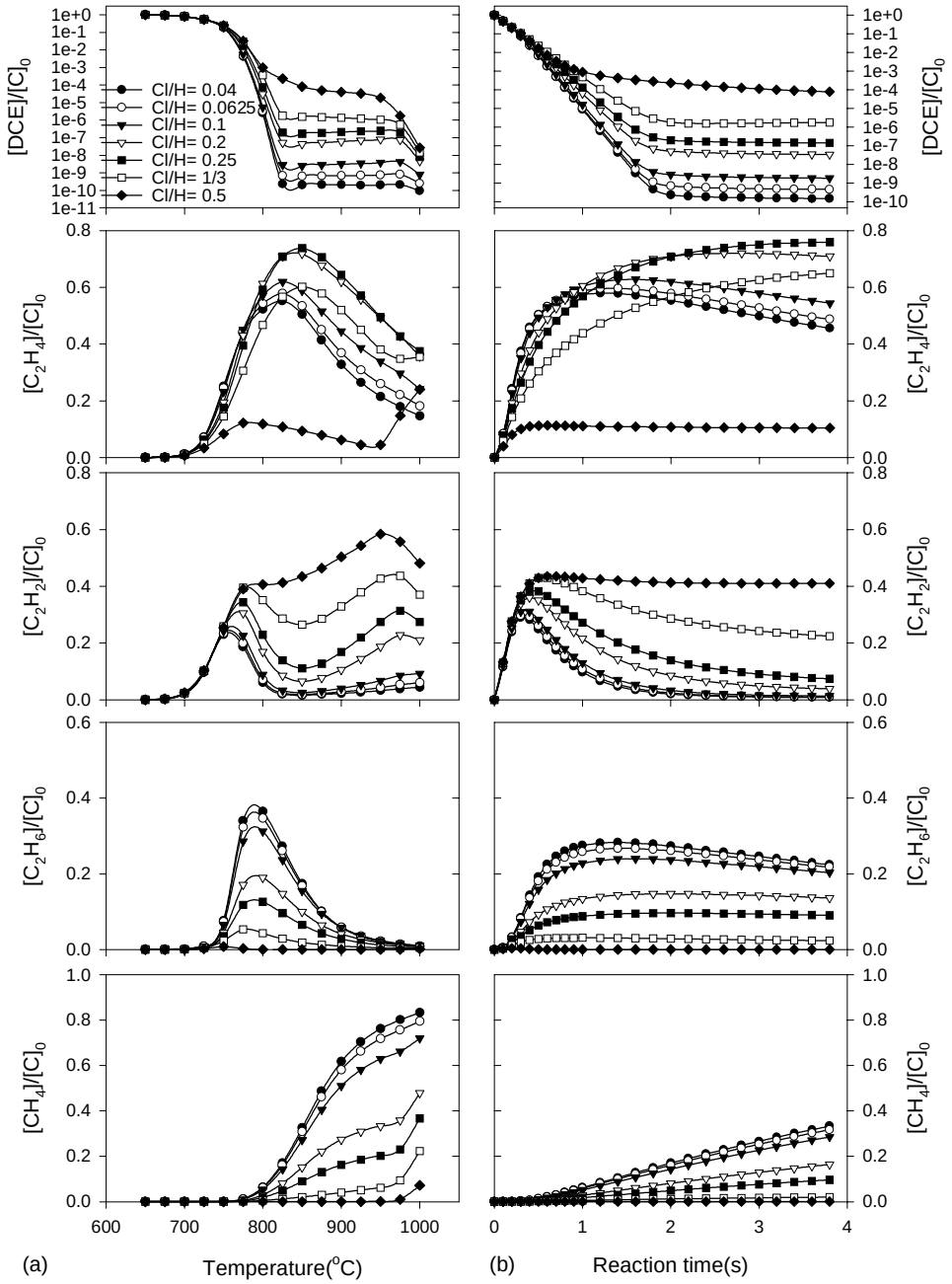

Fig. 12. The concentration profiles of DCE, C_2H_4, C_2H_2, C_2H_6, and CH_4 from the model prediction for DCE: H_2 = 1:24, 1:15, 1:9, 1:4, 1:3, 1:2, and 1:1. (a) Profiles as a function of temperature at 2.0 s and (b) profiles as a function of reaction time at 825 °C.

the results of this analysis, assuming that C_2H_4 is the subject of production, we suggest that the optimal condition for the pyrolysis of DCE in H_2 is DCE:H_2 = 1:3 at 825 °C and 2.0 s.

4. Conclusions

The reaction of excess hydrogen with CH_2CCl_2 was studied in a tubular flow reactor at 1 atm and from 575 to 900 °C. The global Arrhenius equation of CH_2CCl_2 is: $k = 4.95 \times 10^{22} \exp(-52.9 \times 10^3/T)$ (s^{-1}). The major products in this study included C_2H_3Cl, C_2H_4, C_2H_2, C_2H_6, CH_4, and HCl, and the number and quantity of chlorinated hydrocarbons products decreased with increasing temperature. Some minor intermediate reaction products, such as C_2HCl, CH_2Cl_2, CHClCHCl, C_4H_{10}, C_6H_6, and C_6H_5Cl, were found.

A detailed reaction mechanism containing 59 species and 202 elementary reactions was assembled. The model was used to compare calculated concentrations with experimental values and agreement was satisfactory for major species involving a reduction by H_2. The sensitivity analysis shows that $CH_2CCl_2 \rightarrow CH_2CCl+Cl$, $CH_2CCl_2+H \rightarrow CH_2CCl+HCl$ and $CH_2CCl_2+H \rightarrow C_2H_3Cl+Cl$ are the primary reactions responsible for the decomposition of CH_2CCl_2. The optimal reaction condition for the C_2 hydrocarbons production from a CH_2CCl_2/H_2 reaction system is recommended as 825 °C and 2 s with $CH_2CCl_2/H_2 = 0.25$.

Acknowledgements

Y.P. Wu gratefully acknowledges funding from National Science Council of ROC (NSC-90-2214-E-197-002).

References

[1] J.I. Baker, R.A. Hites, Environ. Sci. Technol. 34 (2000) 2879.
[2] B.K. Gullett, A. Touati, C.W. Lee, Environ. Sci. Technol. 34 (2000) 2069.
[3] A.M. Mastral, M.S. Callen, Environ. Sci. Technol. 34 (2000) 3051.
[4] K. Li, E.M. Kennedy, B. Moghtaderi, B.Z. Dlugogorski, Environ. Sci. Technol. 34 (2000) 584.
[5] M.R. Booty, J.W. Bozzelli, W. Ho, R.S. Magee, Environ. Sci. Technol. 29 (1995) 3059.
[6] R. Louw, H. Dijks, P. Mulder, Chem. Ind. 19 (1983) 759.
[7] Y.S. Won, J.W. Bozzelli, Combust. Sci. Tech. 85 (1992) 345.
[8] S.C. Chuang, J.W. Bozzelli, Environ. Sci. Technol. 20 (1986) 568.
[9] Y.S. Won, S.P. Choi, J. Korean Soc. Environ. Eng. 17 (1995) 167.
[10] J.A. Manion, R. Louw, J. Chem. Perk. Trans. 2 (1988) 1547.
[11] P.H. Taylor, D.A. Tirey, B. Dellinger, Combust. Flame 104 (1996) 260.
[12] W. Tsang, J.A. Walker, In: Proceedings of the 23rd Symposium (International) on Combustion, Pittsburgh, 1990, p. 139.
[13] Y.P. Wu, Y.S. Won, Combust. Flame 122 (2000) 312.
[14] Y.P. Wu, Y.F. Lin, C.L. Huang, Fuel submitted.
[15] Y.P. Wu, Y.F. Lin, J. Hazard. Mater. B91 (2002) 239.
[16] Y.P. Wu, Y.F. Lin, Aerosol Air Quality Res. 1 (2001) 91.
[17] W.C. Gardiner Jr. (Ed.), Gas-Phase Combustion Chemistry, Springer, New York, 1999.
[18] D.L. Allara, R.J. Shaw, J. Phys. Chem. 78 (1974) 232.

[19] National Institute of Standard and Technology Standard Reference Database 17, 1992.
[20] G.P. Smith, D.M. Golden, M. Frenklach, N.W. Moriarty, B. Eiteneer, M. Goldenberg, C.T. Bowman, R.K. Hanson, S. Song, W.C. Gardiner, Jr., V.V. Lissianski, Z. Qin, http://www.me.berkeley.edu/gri_mech/.
[21] S.W. Benson, Thermochemical Kinetics, Wiley, New York, 1976.
[22] A.M. Dean, J.W. Bozzelli, E.R. Ritter, Combust. Sci. Technol. 80 (1991) 63.
[23] R.J. Kee, F.M. Rupley, J.A. Miller, CHEMKIN-II Computer Code, SAND89-8009B, UC-706, Sandia National Lab, Livermore, CA, 1989.
[24] JANAF Thermochemical Table, third ed., NSRDS-NBS 37, 1986.
[25] D.R. Stull, E.F. Westrun, G.C. Sinke, The Chemical Thermodynamics of Organic Compounds, Robert E. Krieger Publishing Co., Florida, 1987.
[26] J.B. Pedley, R.D. Naylor, S.P. Kirby, Thermochemical Data of Organic Compounds, second ed., Chapman and Hall, London, 1986.
[27] E.R. Ritter, J.W. Bozzelli, Int. J. Chem. Kinet. 23 (1991) 767.
[28] A.E. Lutz, R.J. Kee, J.A. Miller, SENKIN: A Fortran Program for Predicting Homogeneous Gas Phase Chemical Kinetics with Sensitivity Analysis, Sandia National Laboratories Report SAND 87-8248, 1987.